Covariance of lucky images for increasing objects contrast: diffraction-limited images in ground-based telescopes

Manuel P. Cagigal,[1][*] Pedro J. Valle,[1][*] Carlos Colodro-Conde,[2] Isidro Villó-Pérez[2][*] and Antonio Pérez-Garrido[3]

[1]*Departamento de Física Aplicada, Universidad de Cantabria Avenida de los Castros s/n, E-39005 Santander, Spain*
[2]*Dpto. Electrónica, Universidad Politécnica de Cartagena, Campus Muralla del Mar, E-30202 Cartagena, Murcia, Spain*
[3]*Dpto. Física Aplicada, Universidad Politécnica de Cartagena, Campus Muralla del Mar, E-30202 Cartagena, Murcia, Spain*

ABSTRACT

Images of stars adopt shapes far from the ideal Airy pattern due to atmospheric density fluctuations. Hence, diffraction-limited images can only be achieved by telescopes without atmospheric influence, e.g. spatial telescopes, or by using techniques like adaptive optics or lucky imaging. In this paper, we propose a new computational technique based on the evaluation of the COvariancE of Lucky Images (COELI). This technique allows us to discover companions to main stars by taking advantage of the atmospheric fluctuations. We describe the algorithm and we carry out a theoretical analysis of the improvement in contrast. We have used images taken with 2.2-m Calar Alto telescope as a test bed for the technique resulting that, under certain conditions, telescope diffraction limit is clearly reached.

Key words: atmospheric effects – techniques: high angular resolution – techniques: image processing.

1 INTRODUCTION

Atmospheric effects affecting the image quality of a ground-based telescope has been a common topic in astronomy for years. The angular resolution of astronomical images from large optical telescopes is usually limited by the blurring produced by refractive index fluctuations through Earth's atmosphere. The development of different techniques like speckle interferometry (Weigelt & Wirnitzer 1983) and speckle masking first or adaptive optics (AO) later has allowed us to almost recover the telescope diffraction limit (Hardy 1998).

An alternative to these techniques is the luckyimaging (LI) technique which was first discussed in depth by David Fried (Fried 1978). The technique consists on taking a series of short-exposure images and then selecting the best ones, i.e. those images with best Strehl ratio. As the atmospheric fluctuations are random, one expects that these fluctuations to be occasionally arranged in such a way as to produce a diffraction-limited image, being of main importance to chose a good criterion for the selection of the best images from the series.

For medium-sized telescopes, the LI technique seems to be very promising because of its low complexity and costs in terms of hardware. Furthermore, LI works with reference stars fainter than those required for the natural guide star AO technique.

The main handicap when using LI is related to the temporal evolution of atmospheric turbulence. The decorrelation time-scale of the atmosphere in the case of LI is about 30 ms (atmospheric coherence time). Hence, exposure times employed with LI technique must be shorter than this coherence time to freeze the atmospheric evolution.

Under this conditions we obtain a distorted PSF whose shape depends on D/r_0, the ratio between the telescope diameter (D) and the Fried parameter r_0, which is the atmospheric coherence length. The number of speckles appearing over the PSF is roughly given by $(D/r_0)^2$ and they are randomly distributed over a circular region of the image with angular diameter λ/r_0.

It must be taken into account that r_0 depends on the detection wavelength (or band) and consequently the number of speckles and the area covered by them are strongly dependent on the wavelength as well. In general, a good balance for high-resolution observations is found observing at *I*-band (700–800 nm wavelength) with a 2.5-m diameter telescope.

In this paper, we propose a new algorithm which takes advantage of temporal atmospheric fluctuations to uncover possible companions surrounding main stars. As we will see later, the intensity of all the pixels where a faint companion is placed will fluctuate in phase with the main star intensity along the image series. However, the pixels containing incoherent speckles will fluctuate in counter phase. Hence, the finding of pixels in the image series which are fluctuating in phase with pixels gathering light from the main star is a method for a robust detection of hidden objects. This goal is accomplished by evaluating the normalized covariance (also known

[*] E-mail: manuel.perezc@unican.es (MPC); pedro.valle@unican.es (PJV); Isidro.Villo@upct.es (IV-P)

as the correlation function) between the main star and the rest of the image pixels along the selected LI series. The result is a kind of bidimensional covariance map so that the pixel intensity is the normalized covariance value. The resulting map is, obviously, normalized to unity. This technique can be applied either for extracting undetected faint companions from the background or to improve spatial resolution of images with detected companions to a main star. In this paper, we define the principles of the COELI algorithm and perform an estimation of the expected contrast of one object placed in the proximities of a main star.

We test the COELI technique with a set of LI images of GJ822 taken at the *I*-band by the 2.2-m diameter Calar Alto telescope. Starting from the experimental LI series, we simulate a double star with different relative intensities and distances. By applying COELI, we are able to detect the presence of point-like sources in regions where the primary halo dominates. In some cases, two stars as close as $1.22\lambda/D$, the telescope diffraction limit, can be resolved.

2 THE COELI ALGORITHM

The image of a point source obtained by a perfect optical system can be described by the Airy pattern. However, in ground-based telescopes where the atmosphere refractive index inhomogeneities distort the incoming wavefront, this image consists of a central peak surrounded by a number of speckles whose temporal average is commonly known as halo. The central peak is formed by the coherent part of the energy at the incoming wavefront added to an incoherent halo while the surrounding speckle is only due to the incoherent wavefront energy. The amount of coherent energy depends on the D/r_0 value. Hence, to increase the central peak energy it is enough to have a less aberrated incoming wavefront or to compensate it by an AO system. In this analysis, we will not consider the use of any AO system, since in that case the intensity statistics will depend on the position at the final image plane (Cagigal, Canales & Oti 2004). Hence, when imaging a distant star, the total star peak intensity would be $i_{sp} = i_{cp} + i_h$, where i_{cp} is the coherent part of the star peak intensity and i_h is the halo peak intensity. The coherent part will increase as the phase variance of the incoming wavefront σ^2 decreases (Hardy 1998; Cagigal & Canales 2000; Canales & Cagigal 1999).

$$i_{cp} = e^{-\sigma^2} \tag{1}$$

while the halo peak intensity i_h evolves as

$$i_h \simeq \frac{1 - e^{-\sigma^2}}{(D/r_0)^2} \tag{2}$$

The total intensity has been normalized to unity. We can see that the halo intensity behaves anticorrelated with intensity of the reference star peak.

Combining equations (1) and (2) we obtain that the height of the coherent peak is the same as that of the surrounding speckles for about $D/r_0 = 8$. The technique we propose here is limited to D/r_0 values ranging under that limit. In a good observing site, a standard r_0 would be around 20 cm. If the technique of LI is applied for selecting the best frames, effective r_0 values of around 30 cm can be reached. This means that, keeping the restriction $D/r_0 = 8$, the suitable telescope diameter would have around 2.4 m of diameter.

If we apply the LI technique for obtaining a short-exposure frame series, the central peak intensity of a star will evolve along the frame series in counter phase with respect to the surrounding halo intensity. This behaviour will be the same for any other object contained in the scientific image. Hence, the intensity value of those pixels
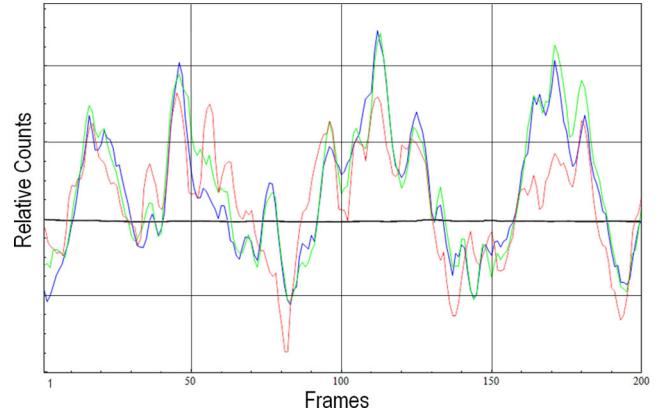

Figure 1. Example of experimental correlations in GJ822. Host star peak intensity (blue line), companion intensity (green line), the inverse of the averaged intensity in an area surrounding the central peak (red line) and the background (black line).

containing the central peak of an astronomical object will oscillate in phase, while the pixels containing the speckled halo will oscillate in counter phase with respect to the peak intensities. As an example, Fig. 1 shows experimental curves for the object GJ822 corresponding to the LI experiment that is described in detail later. The host star peak intensity (blue line), the companion intensity (green line), the inverse of the averaged intensity in an area surrounding the central peak (red line) and the background (black line) are plotted once normalized for a series of LI frames. It can be seen that there exists a strong correlation between the host star and companion intensities. The correlation between the host star intensity and the inverse of the average halo intensity is also evident. The noise background remains basically constant along the frame series. It is evident that while all the objects fluctuate in phase along the frame series, their corresponding halo fluctuate in counter phase.

COELI basically consists of the calculation of the covariance between the main star peak intensity and the intensity of the rest of the pixels forming the image. This covariance is estimated using a series of short-exposure lucky images. The result is a covariance map where each pixel of the map contains the value of its covariance with respect to that of the main star. The normalized covariance values will range from 1, corresponding to the reference star, to -1 for those pixels fluctuating in counter phase with respect the main star.

The algorithm is composed by the following steps.

(1) To obtain accurate covariance estimate we have to re-centre the image series. For an efficient centring, we have choose the superimposition of the most intense pixel of every frame.

(2) The second step is to eliminate intensity background pixels with slow spatial dependence. To accomplish that we convolved the frame series with a 1 pixel radius Laplacian filter (Gonzalez & Woods 2002). This kind of filters are commonly known as point detectors.

(3) After this simple preprocessing it is possible to estimate the normalized covariance (Pearson correlation) between the most intense peak of the reference star and the rest of the frame pixels along the frame series.

The procedure we followed was to calculate the normalized covariance given by the expression:

$$C[i_{sp}, i(r)] = \frac{\text{Conv}[i_{sp}, i(r)]}{\sigma_{sp} \, \sigma_{ir}} \tag{3}$$

and the convolution, given by

$$\text{Conv}[i_{\text{sp}}, i(r)] = <i_{\text{sp}}\, i(r)> - <i_{\text{sp}}><i(r)> \qquad (4)$$

where i_{sp} stands for the star peak intensity, $i(r)$ is the intensity detected at a position r from the star peak $[r = (i, j)]$, σ is the standard deviation and $<>$ is the ensemble average (frame series average).

In general, the intensity $i(r)$ is the addition of the star halo background plus noise, $i(r) = i_{\text{h}}(r) + i_{\text{n}}$. However, in those pixels where there is an object it would be necessary to add the object intensity, $i(r) = i_{\text{h}}(r) + i_{\text{n}} + i_o$. The set of values obtained by applying equations (3) and (4) are saved at the corresponding (i, j) pixel position thus forming a normalized covariance map. All the preceding steps have been included in an ImageJ (http://imagej.nih.gov/ij) plugin named COELI.

3 COVARIANCE CONTRAST

To evaluate the capability of this tool for detecting objects, it is necessary to define the contrast of the object against the background at the covariance map estimated using equation (3).

To accomplish this task we define the object peak intensity i_o, which is proportional to i_{sp}:

$$i_o = k_o i_{\text{sp}} \qquad (5)$$

The star peak intensity (i_{sp}) can be obtained as the addition of the coherent peak intensity (i_{cp}) plus the intensity star halo at the centre (i_{h}):

$$i_{\text{sp}} = i_{\text{cp}} + i_{\text{h}} \qquad (6)$$

The intensity star halo is a function of the distance to the main star and it is related to i_{cp} through the expression:

$$i_{\text{h}}(r) = k(r)(1 - i_{\text{cp}}), \qquad (7)$$

where $k(r)$ is a function which states the halo intensity spatial dependence. Finally, the readout noise intensity is given by i_{n}. The normalized covariance between the central star peak, i_{sp}, and pixels inside the halo is given by

$$C(i_{\text{sp}}, i_{\text{h}} + i_{\text{n}}) = \frac{-k\sigma_{\text{cp}}^2 + \sigma_{\text{h}}^2}{\sigma_{\text{sp}}\sqrt{\sigma_{\text{n}}^2 + \sigma_{\text{h}}^2}} \qquad (8)$$

Where we have used equation (7) for obtaining an approximated expression of the covariance between i_{sp} and i_{h} (the explicit dependence with position r has been omitted). The covariance between the central star peak and those halo pixels containing an object will be

$$C(i_{\text{sp}}, i_{\text{h}} + i_{\text{n}} + i_o) = \frac{(-k + k_o - kk_o)\sigma_{\text{cp}}^2 + \sigma_{\text{h}}^2}{\sigma_{\text{sp}}\sqrt{\sigma_o^2 + \sigma_{\text{n}}^2 + \sigma_{\text{h}}^2}} \qquad (9)$$

It is interesting to note that we have considered the reading noise intensity at the star peak position negligible compared to the other noises affecting the measurement. Hence, the covariance contrast between pixels containing an object and those without object for pixels inside the halo can be defined by the quotient of equations (9) and (8):

$$\text{Contrast}(r) = \frac{\left[(-k + k_o - kk_o)\sigma_{\text{cp}}^2 + \sigma_{\text{h}}^2\right]\sqrt{\sigma_{\text{n}}^2 + \sigma_{\text{h}}^2}}{(-k\sigma_{\text{cp}}^2 + \sigma_{\text{h}}^2)\sqrt{\sigma_o^2 + \sigma_{\text{n}}^2 + \sigma_{\text{h}}^2}} \qquad (10)$$

where σ_x^2 is the variance corresponding to the intensity i_x. We build up a covariance contrast map evaluating this expression for all the pixels of the image. As it can be seen, the contrast of one object at the halo estimated from the covariance map will depend on a series of parameters (k_o, and k) and variances (σ_{sp}^2, σ_h^2, σ_o^2 and σ_n^2). To estimate the value of the expected contrast we will use some approximated expressions for the different variances.

An approximated expression for the variance of the peak intensity i_{sp} has already been evaluated for astronomical images (Gladysz & Christou 2009; Yaitskova, Esselborn & Gladysz 2012) as

$$\sigma_{\text{sp}}^2 = \frac{2}{N} <i_{\text{sp}}> \left[1 - <i_{\text{sp}}>\right]^2 \qquad (11)$$

where N is the number of homogeneous areas in the telescope pupil and can be approximated by

$$N = \left(\frac{D}{r_0}\right)^2 \qquad (12)$$

In low light level it is necessary to include the variance due to the Poissonian detection process which is equal to the intensity mean value:

$$\sigma_{\text{sp}}^2 = \frac{2}{N} <i_{\text{sp}}> \left[1 - <i_{\text{sp}}>\right]^2 + <i_{\text{sp}}> \qquad (13)$$

On the other hand, we can consider that the halo variance comes from the speckle statistics as Aime et al. suggested (Aime & Soummer 2004a,b):

$$\sigma_{\text{h}}^2 = i_{\text{h}}^2 + 2i_{\text{cp}}i_{\text{h}} + i_{\text{cp}} + i_{\text{h}} \qquad (14)$$

Where we have not considered the radial dependence of the halo intensity but the variance due to the Poissonian detection process ($\sigma_{\text{p}}^2 = i_{\text{cp}} + i_{\text{h}}$) has been included.

Hence, the coherent peak variance can be obtained from the difference of the previous ones:

$$\sigma_{\text{cp}}^2 = \sigma_{\text{sp}}^2 - \sigma_{\text{h}}^2 \qquad (15)$$

Finally, we shall assume that the object adds a constant value in one pixel and its variance is only due to the Poissonian detection process (Aime & Soummer 2004a). Therefore, the variance of a companion of intensity i_o will be

$$\sigma_o^2 = <i_o> \qquad (16)$$

The detection noise variance σ_{n}^2 is not estimated since the analysis will be performed as a function of its possible values.

4 CONTRAST ANALYSIS

The purpose of the COELI algorithm is to increase the visibility of the objects whose light suffers a temporal oscillation which is in phase with that of the reference star. Hence, it can be applied for extracting a faint companion from a noisy background. The only limitation relies on the noise level affecting the companion intensity measurement. If the light intensity of the pixel where a companion is located is clearly dominated by the noise, the COELI algorithm will consider that in the pixel there is not any object. Hence, the detection noise reduction (cameras with small electronic noise, camera cooling, etc.) will allow faint objects to appear.

As an example, let us consider a main star with a Strehl of 0.1 corresponding to $D/r_0 = 5.5$. We estimate the contrast corresponding to a companion with an intensity equal to a half of the main star intensity ($k_o = 0.5$) placed near to the peak star, so that we can use the following approximated expression for evaluating the halo height, $i_{\text{h}} \propto (r_0/D)^2$ (Hardy 1998; Cagigal & Canales 2000). Fig. 2 shows the covariance curves corresponding to equations (8) and (9)
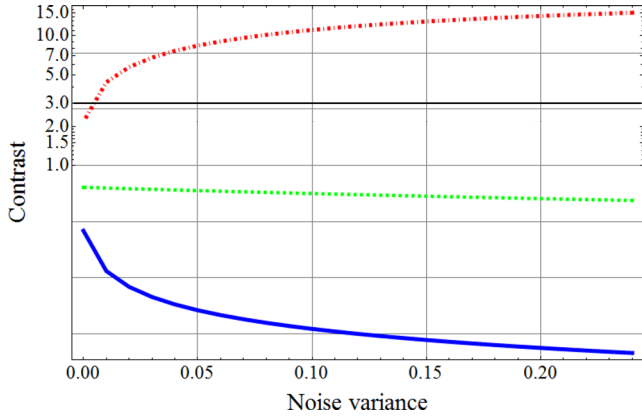
Figure 2. Contrast (red dot–dashed line), background covariance (blue solid line) and background plus object covariance (green dashed line) as a function of the detection noise variance. Black line indicates a reference contrast value of 3.

along with that of the contrast, equation (10) as a function of the noise variance. To evaluate the curves the approximated variances of equations (12)–(16) have been used. It can be seen that the contrast (red line) tends very quickly to a value of 5 as the reading noise increases, since the covariance drops significantly in those pixels where there is not any object (blue line) while it keeps almost a constant value in the pixel where the object is present (green line).

5 EXPERIMENTAL CHECKING

To check the COELI technique a series of experimental measurements were completed. The observations were carried out during 2013 September using Astralux at the 2.2-m Telescope at CAHA (Almería, Spain). This instrument incorporates a fast readout electron multiplying CCD chip (EMCCD) which is able to acquire images with a very low readout noise thanks to internal charge amplification before conversion to voltage by an output amplifier. Astralux allows the acquisition of a large number of images, typically several thousand for each target, with exposure times about a few tens of milliseconds. Images that clearly show frozen atmospheric speckles. Conventional large integration times average all of these speckles, which yields to the usual seeing-limited point spread functions with a seeing dependent on atmospheric perturbations.

The observations were done in SDSS I band with a pixel scale of 47 mas pixel^{-1} and 7000 images were acquired, each with exposure time of 30 ms. The internal electron multiplying gain was adopted to work in the EMCCD linear regime and therefore determined by the luminosity of the target. To carry out a precise calibration of the pixel scale and camera rotation we observed the core of the globular clusters M15, and correlated the astrometric data with catalogues from *Hubble Space Telescope*. This provided an accurate astrometric calibration for each observing night with plate scale precision as good as 0.01 mas. The main source of astrometric error for a given star results from the uncertainty in the measurement of the barycenter which is in turn mainly determined by the signal-to-noise ratio. In our data this uncertainty is typically 0.1 pixel and reaches 0.2 in the faintest stars. This leads to typical errors in separation of the order of 10 mas.

To check if our algorithm can reduce the main star halo without affecting the detectability of other fainter objects, we selected the 100 frames of to the object GJ822 with highest Strehl. Fig. 3(a) shows the result of applying a shift-and-add algorithm (SAA) to the
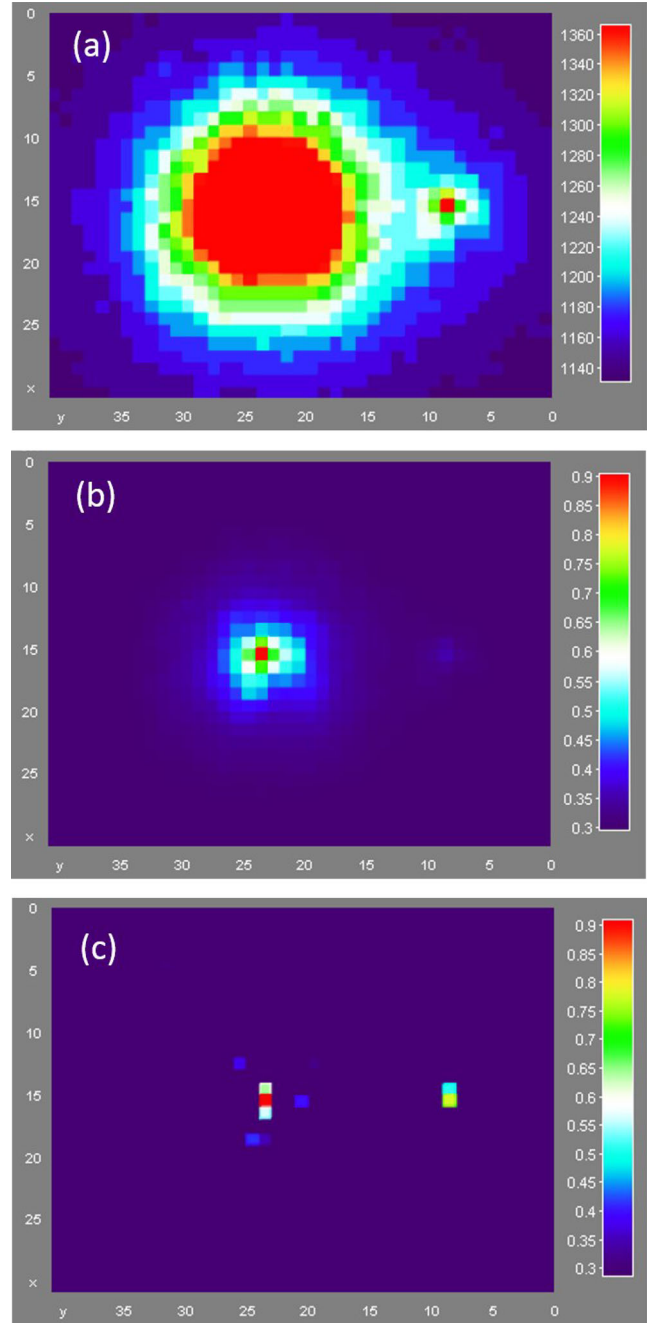

Figure 3. (a) Plot obtained after applying SAA to the 100 best frames of the object GJ822, the grey level scale has been chosen to allow the image of the companion to be visible. (b) Same SAA image but normalized to its peak value. (c) Plot after applying COELI to the same stack.

stack. In this figure, the chosen scale allows the 30 times fainter companion to appear. When the image is scaled to normalize the peak high, the companion disappears (Fig. 3b). We have already applied COELI to the same 100 frames stack obtaining the image shown in Fig. 3(c). It can be seen that a drastic halo reduction has happened while the secondary object is maintained. We can also see that the photometry has been complete lost since what Fig. 3(c) is showing is only the covariance map of the image stack with respect to the central star.

We have seen that COELI is able to improve the visibility of faint objects but, at the same time, it is very effective suppressing
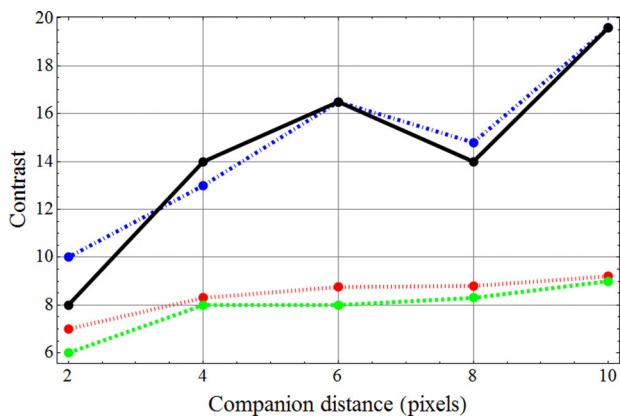
Figure 4. Contrast at the covariance map as a function of the distance between companion and main star. The companion intensity is a half of that of the main star. Contrast reached using only once the Laplacian filter with radius one (green dashed line) and two pixels (red dotted line) and that reached using twice the Laplacian filter with radius one (blue dot–dashed line) and two (black solid line) pixels.

the speckle halo surrounding the star coherent peak, since the halo oscillates in counter phase with respect to the peak. This result shows the feasibility of the algorithm to resolve companions to main stars with angular separations close to the telescope diffraction limit.

6 RESOLUTION ANALYSIS

Our aim in this section to measure the ability of the algorithm to resolve objects with small angular separations. Let us consider two punctual sources with an angular size given by the diffraction theory. The central peak angular radius is given by $1.22\lambda/D$, where λ is the detection wavelength and D the telescope pupil diameter. The Rayleigh criterion establishes that two punctual sources are considered as resolved when the principal diffraction maximum of one image coincides with the first minimum of the other. Only perfect optical systems are able to meet the Rayleigh criterion but when an aberrating medium is introduced it may be impossible. In particular, to reach diffraction limited images in ground-based telescopes, where the light coming from the stars has to go across the atmosphere, the telescope size has to be similar to the Fried parameter. Recently, some successful results have been reported applying AO to a medium size (1.5 m) telescope (Serabyn, Mawet & Burruss 2010). Our goal is to reach diffraction limited images using only a post-processing technique to lucky images detected in a 2.2-m telescope.

We have already shown that before applying the correlation algorithm given by equation (3) it is necessary to improve the object contrast by passing a Laplacian filter. However, this raises a number of questions. For example, the dependence of the contrast on the radius of the applied mask or the number of mask iterations required. To answer these questions, we have carried out a simulation using an experimental stack containing the 100 best frames obtained from the previously described experiment. We have duplicated it, translated it a number of pixels and multiplied it by a reducing coefficient. This modified stack is added to the unmodified one to create a double object. We have repeated the same process for different displacements and different reducing coefficient values. This simulation technique has been widely used for simulating binary stars (Bagnuolo 1982; Lee & Yee 2003).

Fig. 4 shows the contrast (ratio between the object covariance and the covariance average value of the surrounding area) as a
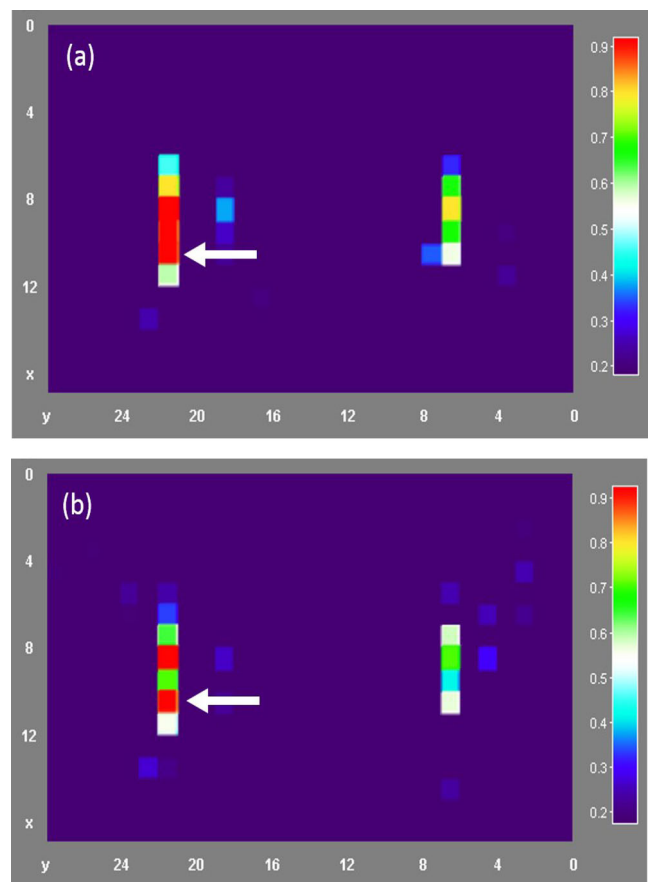

Figure 5. Covariance map for two objects placed at a distance of two pixels and with a relative intensity of 0.7. (a) The 1 pixel Laplacian mask has been applied once, (b) the 1 pixel Laplacian has been convolved twice.

function of the distance in pixels between the two objects when the companion intensity is a half of that of the main star. It can be seen that when the Laplacian filter is convolved with the image stack only once before applying the covariance estimating algorithm the result is almost identical for a mask radius of one and two pixels (green and red curves, respectively). When a Laplacian filter is convolved twice with the stack the result is independent of the filter radius too (blue and yellow curves, respectively) and clearly improves the contrast obtained with only one convolution. We have already checked that a third convolution with the Laplacian mask does not improve the result obtained with only two convolutions.

As an example we have compared the covariance map obtained for the objects placed two pixels apart and with relative intensity of 0.7. The result clearly depends on the number of times the 1 pixel radius Laplacian mask has been convolved before applying the covariance calculation. In Fig. 5(a), where we have convolved the Laplacian mask only once, we can see a broad object that suggests a double star (marked with a white arrow). However, the image is noisy and it is difficult to make a decision. Fig. 5(b) is the same case but now the Laplacian mask has been convolved twice. The noise has been drastically reduced and we can see that the broad object we had in Fig. 5(a) is now split into two different ones.

Another interesting point is the contrast dependence on the relative intensity of the object. To check this, we have used the same stack as before for evaluating the attainable contrast for different intensity ratios. As a result of Fig. 4, to evaluate the dependence of the contrast on the relative intensity we have convolved the image
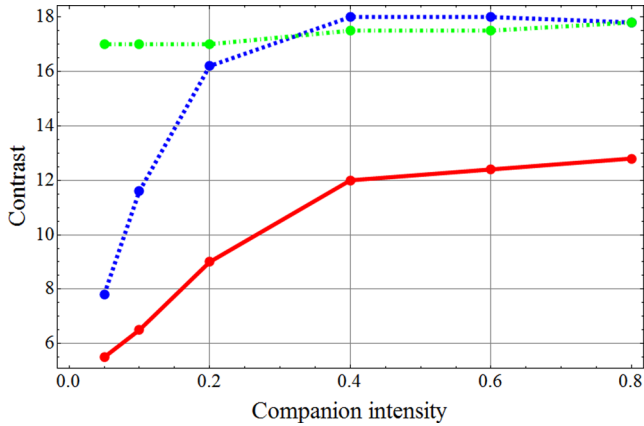
Figure 6. Contrast as a function of the companion intensity for a distance between companion and main star of 2 (red solid line), 5 (blue dashed line) and 20 pixels (green dot–dashed line).

stack twice with a 1 pixel radius Laplacian filter before applying the covariance algorithm.

Fig. 6 shows that there is a general behaviour; the contrast increases when the companion intensity or the distance between objects increases. In particular, the curve shows that objects as close as two pixels, which is the diffraction limit of our telescope according to the Rayleigh criterion, can be resolved. However, for this particular case, only when the companion intensity is larger than 0.1 times that of the main star the contrast is above the 5σ value required for detection.

Fig. 7(a) shows SAA result for a series of images containing two objects with a relative intensity of 0.6 and a relative distance of two pixels. Fig. 7(b) shows COELI result for the same image series. Fig. 7(c) shows SAA result for two objects with a relative intensity of 0.8 and a relative distance of two pixels and Fig. 7(d) shows COELI result for the same image series. By comparing Fig. 7(a) and (b), we see that the companion clearly appears when using COELI while SAA provides a single peak. The same result is reached by comparing Fig. 7(c) and (d). This comparison states the advantage of using COELI for detecting objects inside the speckled halo. Relative intensity between main star and companion is a key factor for companion detection. For a relative intensity of 0.6 and a relative distance of two pixels we can clearly distinguish between the two objects (Fig. 7b). However, when the relative intensity is 0.8 it is difficult to distinguish them as Fig. 7(d) shows.

7 CONCLUSIONS

We have introduced a new technique based on the estimation of the covariance of the intensity applied over a series of lucky images. This technique takes advantage of the fact that the two components of the image of an astronomical object, coherent central peak and speckled halo, have intensities that oscillate in counter phase. We have shown how to evaluate the covariance map and how different noises involved in the image detection may affect the covariance map estimate. We have checked the COELI algorithm using actual lucky images taken at the 2.2-m CAHA telescope.

We have seen that the application of our technique allows the speckled halo to be extremely reduced, which allows very close companions to be detected. In fact, we show that the diffraction limit of the telescope has been achieved under certain conditions of relative intensity between objects.
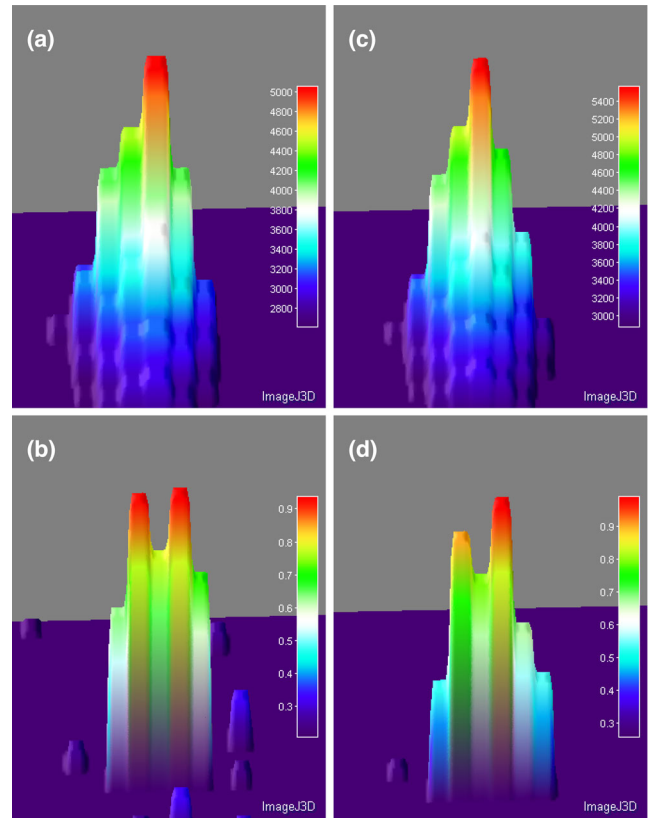
Figure 7. Images corresponding to two objects placed at a distance of two pixels. The relative intensity is 0.6 for (a) (obtained by SAA) and (b) (obtained by COELI). The relative intensity is 0.8 for (c) (obtained by SAA) and (d) (obtained by COELI).
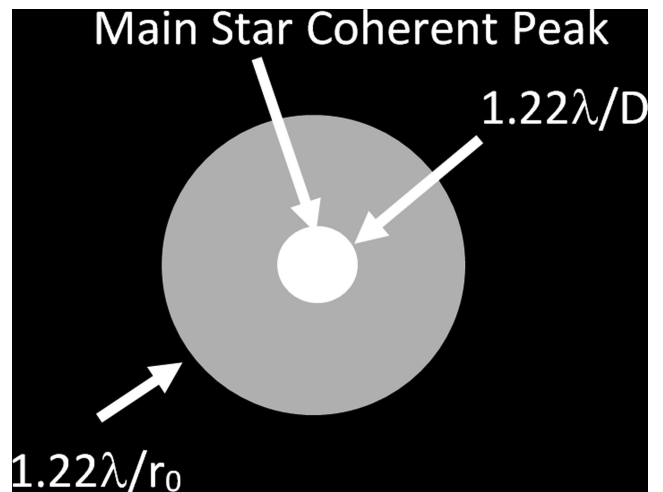

Figure 8. The area of applicability is found between the first Airy ring ($1.22\lambda/D$) and the outer radius $1.22\lambda/r_0$ corresponding to the speckled halo limit.

Since the COELI technique cancel out the speckled halo surrounding the coherent peak of the main star, the technique is particularly effective in the area covered by the halo. Fig. 8 shows a plot of the area of interest with an outer radius of $1.22\lambda/r_0$, which is equivalent to D/r_0 times the Airy ring radius. As we stated previously, the limiting D/r_0 value for applying COELI is about 8. Hence, the

detection area is an annulus with inner radius of $1.22\lambda/D$ and outer radius about 8 times the inner one.

A clear limiting factor for applying this technique is the detection noise affecting the captured images. Theoretical analysis shows that the lower camera noise the better achievable contrast, as it could be expected.

We have experimentally checked that COELI detects all the successive images of the main star caused by misalignment of the optical set up. Hence, this technique could also be an effective tool for detecting set up misalignment prior to use it for capturing scientific images.

A drawback of the technique is that it does not maintain the photometry since what we obtain is not an image any more, but a map of covariance values.

Nevertheless, we consider that this technique may be considered as an interesting tool for reaching telescope diffraction limit from ground-based telescopes with sizes under 2.5 m. Besides, it has the additional advantage of a much reduced cost, in particular when compared with AO.

ACKNOWLEDGEMENT

REFERENCES

Aime C., Soummer R., 2004a, in Hlawatsch F., Matz G., Rupp M., Wistawel B., eds, European Signal Processing Conf., 1071 Influence of Speckle and Poisson Noise on Exoplanet Detection With a Coronagraph. Vienna, Austria

Aime C., Soummer R., 2004b, ApJ, 612, L85

Bagnuolo W. G., Jr, 1982, MNRAS, 200, 1113

Cagigal M. P, Canales V. F., 2000, J. Opt. Soc. Am. A., 17, 903

Cagigal M. P., Canales V. F., Oti J. E., 2004, PASP, 116, 965

Canales V. F., Cagigal M. P., 1999, J. Opt. Soc. Am. A, Vol. 16, No. 10

Fried D. L., 1978, J. Opt. Soc. Am., 68, 1651

Gladysz S., Christou J. C., 2009, ApJ, 698, 28

Gonzalez R. C., Woods R. E., 2002, Digital Image Processing. Prentice Hall, New Jersy

Hardy J. W., 1998, Adaptive Optics for Astronomical Telescopes. Oxford Univ. Press, Oxford

Lee B. L., Yee H. K. C., 2003, in Deming D., Seager S., eds, ASP Conf. Ser. Vol. 294, Photometric Simulation of Transiting Extrasolar Planets Scientific Frontiers in Research on Extrasolar Planets. Astron. Soc. Pac., San Francisco, p. 413

Serabyn E., Mawet D., Burruss R., 2010, Nature, 464

Weigelt G., Wirnitzer B., 1983, Opt. Lett., 8, 389

Yaitskova N., Esselborn M., Gladysz S., 2012, Proc. SPIE, 8447, 223

This paper has been typeset from a TEX/LATEX file prepared by the author.